JOURNAL OF ENVIRONMENTAL PROTECTION SCIENCE (2009), Vol. **3**, pp. 1 – 10.

Adsorption of methylene blue onto gulmohar plant leaf powder: Equilibrium, kinetic, and thermodynamic analysis

V. Ponnusami, R. Aravindhan, N. Karthik raj, G. Ramadoss, S. N. Srivastava*

School of Chemical & Biotechnology, SASTRA University, Thanjavur, India.

Abstract

Batch adsorption of methylene blue onto gulmohar plant leaf powder (GUL) was investigated. The effects of pH, initial dye concentration, particle size, dosage, agitation speed, and temperature were studied. Langmuir and Freundlich isotherm models were used to test the equilibrium data. The linear regression coefficient R^2 and non-linear regression coefficient $\chi 2$ were used to elucidate the best fitting isotherm model. The Langmuir isotherm was found to be the best fitting isotherm model. The monolayer adsorption capacities of GUL were found to be 120, 178, and 253 mg/g at temperatures of 293, 303, and 313 K, respectively. The pseudo-second order model best fits the adsorption kinetics. The multi-linearity obtained in the intra-particle diffusion plot showed that both external diffusion and internal diffusion resistances are important in controlling the overall adsorption rate. Gibb's free energy values obtained confirmed that the process was feasible and spontaneous (ΔG = -24.44, -23.90, and -22.75 kJ/mol). The value of ΔH (-49.12 kJ/mol) indicated that an exothermic chemisorption had taken place. The value of ΔS (-0.084 kJ/mol) suggested that the randomness decreased after adsorption. High values of q_m indicate that GUL can be a potential substitute for activated carbon.

Keywords: Gulmohar, methylene blue, adsorption, isotherm, kinetics.

JEPS (2009), Vol. **3**, pp. 1 – 10.

1. Introduction

Dyes are used by plastic, paper, tannery, textile, and many other industries to color their end products. A significant portion of the dyes remains unconsumed and, therefore, let out in the effluent. The presence of dyes in aqueous effluents poses a serious ecological threat. It reduces light penetration in water bodies and interferes with metabolic activities of aquatic life.[1] Dyes are mostly resistant to biodegradation and therefore are not removed by conventional treatment techniques. Many dyes and/or their metabolites are known to have carcinogenic, mutagenic, and teratogenic effects on aquatic life and humans.[2] Therefore, it is essential to treat effluents before letting them out. The biological and physical/chemical methods available for the removal of dyes from aqueous effluents include anaerobic/aerobic treatment, coagulation, flocculation, oxidation, ozonation, membrane separation, and adsorption. Among these methods, adsorption has been proven to be more efficient, offering advantages over conventional processes.[3,4] Though activated carbon has been widely used as an adsorbent for the removal of a wide range of organic molecules and metals, high costs and regeneration difficulties hamper large-scale application of activated carbon.[2] This has prompted many researchers to study the feasibility of using low cost substances as alternate adsorbents. Because many agro-wastes are either arbitrarily discarded or set on fire, exploitation and utilization of these materials should bring economic and social benefits to mankind.[2] Materials like neem leaf powder,[5] bagasse fly ash,[6] sugarcane dust,[7] rice husk,[8] banana pith,[9] coir pith,[10] orange peel,[11] shells of bittim,[12] chemically treated guava leaf powder,[13] phoenix tree leaves,[14] citrus grandis,[15] unburned carbon,[16] etc., have been studied. Thus, in the present work, adsorption potential of gulmohar plant leaf powder (GUL) was investigated. Gulmohar is a flamboyant flowering tree (*Delonix regia, Caesalpiniaceae family*). For several weeks in spring and summer it is covered with exuberant clusters of flame-red flowers, 100 to 150 mm across. The delicate, fern-like leaves are composed of small individual leaflets, which fold up at the onset of dusk. Gulmohar grows 10 to 13 m tall, but its elegant wide-spreading

*To whom all correspondence should be addressed: Tel: + 91-99947-12632; Fax: +91-4362-264120; E-mail:vponnu@chem,sastra.edu.

umbrella-like canopy can be wider than its height. Gulmohar is naturalized in India and is widely cultivated as a street tree.

2. Materials and Methods

Mature gulmohar leaves were washed thoroughly with distilled water to remove dust and other impurities. Washed plant leaves were dried overnight at 343 K in a hot air oven. Dried leaves were then ground in a domestic-mixer-grinder. After grinding, the powder was screened in a sieve shaker. Screened powders were again washed and dried. Different sized GULs were then stored in plastic containers for further use.

Methylene blue (MB, chemical formula: $C_{16}H_{18}N_3SCl$; FW: 319.86 g mol^{-1}, λ_{max}= 662 nm, class: thiazine, C.I. Classification Number: 52015) is the most important basic dye. It dissociated into methylene blue cation and chloride anion. Dissociated MB is preferentially adsorbed onto many solids. For this reason, MB was used in the present study. The MB dye was obtained from Ranbaxy Laboratories Limited (India) and used without further purification. The dye is not regarded as acutely toxic, but it can have various harmful effects. On inhalation, it can give rise to short periods of rapid or difficult breathing, while ingestion through the mouth produces a burning sensation and may cause nausea, vomiting, diarrhea, and gastritis.[5] Stock solution was prepared by dissolving the required amount of dye in double distilled water, which was later diluted to required concentrations. All the solutions were prepared in double distilled water. Solution pH was adjusted by adding either 0.1 N HCl or 10% Na_2CO_3 as required. The batch adsorption experiments were carried out by varying initial pH, initial dye concentrations, temperature, adsorbent dosage, particle size, and agitation speed. For each run, accurately weighed GUL was added to 100 cm^3 of aqueous dye solution taken in a 250 cm^3 conical flask and the mixture was agitated in an incubated shaker at constant RPM and temperature. Samples were withdrawn at regular time intervals using a fine tip syringe to minimize carryover of adsorbent particles with the sample. Samples were immediately centrifuged (Remi Research centrifuge) to separate remaining adsorbent particles. Concentrations of the dye solutions were determined by measuring the absorbance of the solution at the characteristic wavelength (λ_{max} = 662 nm) of MB using a double beam UV-Vis. spectrophotometer (Systronics 2201). Samples were diluted if the absorbance exceeded 0.8. Final concentration was then determined from the calibration curve already prepared.

2.1. Equilibrium isotherms

Equilibrium data commonly known as adsorption isotherms are basic requirements for the design of adsorption systems. Langmuir and Freundlich isotherms were used to describe the equilibrium characteristics of adsorption in the present study. The Langmuir isotherm[17] basically assumes homogenous surface energy distribution. The Langmuir isotherm assumes that the adsorption rate is proportional to the number of vacant sites on the adsorbent and fluid phase concentration, while the desorption rate is proportional to the number of sites covered with adsorbate molecules. Thus, at dynamic equilibrium the dye concentration in the solid phase can be expressed as:

$$q_e = q_m \frac{K_L C_e}{1 + K_L C_e} \quad (1)$$

Where:

q_e = equilibrium dye concentration in the solid phase, mg g^{-1}

q_m = maximum monolayer dye concentration in the solid phase, mg g^{-1}

C_e = equilibrium dye concentration in the aqueous phase, mg dm^{-3}

K_L = Langmuir equilibrium constant, mg^{-1} dm^3

Eq. (1) can then be rearranged into linear form as follows:

$$\frac{1}{q_e} = \frac{1}{q_m K_L C_e} + \frac{1}{q_m} \quad (2)$$

By plotting $1/q_e$ versus $1/C_e$, the Langmuir constants q_m and K_L can be obtained. The essential characteristics of the Langmuir isotherm can be expressed by a dimensionless separation parameter, which is defined as:

$$R_L = \frac{1}{1 + K_L C_0} \quad (3)$$

R_L indicates the nature of adsorption. Adsorption is favorable when the value of R_L is between 0 and 1.[18] Another adsorption isotherm commonly used for liquid phase adsorption on a surface having heterogeneous energy distribution is the Freundlich isotherm.[19] It is expressed as follows:

$$q_e = K_F C_e^{1/n} \quad (4)$$

K_F and n are indicators of adsorption capacity and adsorption intensity, respectively.[20] Rearranging Eq. (4) we get:

$$\ln q_e = \ln K_F + \tfrac{1}{n} \ln C_e \quad (5)$$

A plot of ln q_e vs. ln C_e yields a straight line. From the slope and intercept of the plot, n and K_F can be estimated.

The value of the Freundlich constant (n) should lie in the range of 1 to 10 for favorable adsorption.

An accurate isotherm is important for design purposes. Linear regression is commonly used to determine the best fitting model and to determine isotherm constants;[16] however, linearization of a non-linear model leads to different axial settings and hence influences the determination process. To overcome this problem, the non-linear Chi-square (χ^2) test had been proposed as an alternate method of determination.[21, 22] Thus, in the present study both R^2 and χ^2 were used to identify the best fitting isotherm model.

2.2. Adsorption kinetic studies

The transient behavior of the dye sorption process is commonly analyzed using pseudo-first order,[23] pseudo-second order,[24-27] and intra-particle diffusion models.[28] However, the pseudo-first order model could not explain the adsorption of MB onto GUL. Therefore, in the present paper only the pseudo-second order and intra-particle diffusion models are discussed.

2.3. Pseudo-second order model

Ho's most widely used pseudo-second order kinetic model[24-27] is expressed in its linear form as follows:

$$\frac{t}{q_t} = \frac{1}{K_2 q_e^2} + \frac{t}{q_e} \qquad (6)$$

Where:

t = time, min

q_t = dye concentration in the solid phase at time t, mg g^{-1}

K_2 = pseudo-second order rate constant, g mg^{-1} min^{-1}

Values of q_e and K_2 can be obtained from the slope and intercept of the plot t/q_t vs. t.

2.4. Intra-particle diffusion

Weber & Morris proposed the intra-particle diffusion model to explain the transient behavior of dye adsorption. Accordingly, if a plot of dye uptake versus $t^{0.5}$ is a straight line passing through the origin, then the effect of external film resistance is negligible. On the other hand, if the intercept deviates from the origin, this shows the importance of the external film resistance. The value y-intercept is a qualitative measure of film thickness. A multi-linearity of the Weber plot is an indication of the presence of different size pores (micro-, meso-, and nano-pores) in the adsorbent.

2.5. Thermodynamic analysis

The Langmuir isotherm constant, K_L, was used to estimate the thermodynamic parameters Gibbs free energy (ΔG), change in enthalpy (ΔH), and change in entropy (ΔS). Negative ΔG indicates the spontaneity of the adsorption process. ΔH is used to identify the exothermic or endothermic nature of adsorption. A positive value of ΔS indicates increased randomness of adsorbate molecules on the solid surface than in the solution.

The free energy of adsorption (ΔG) can be related with the Langmuir adsorption constant[6] by the following expression:

$$\Delta G = -RT \ln K_L \qquad (7)$$

Also, enthalpy and entropy changes are related to the Langmuir equilibrium constant by the following expression:[6]

$$\ln K_L = \frac{\Delta S}{R} - \frac{\Delta H}{RT} \qquad (8)$$

Thus, a plot of ln K_L vs. $1/T$ should be a straight line. ΔH and ΔS values could be obtained from the slope and intercept of this plot.

3. Results and Discussion

3.1. Effect of initial pH

Initial pH is an important factor that affects adsorption. Effect of pH on adsorption of MB onto GUL was analyzed over a pH range from 2.4 to 9.0. Dye uptake was found to increase with increase in initial solution pH. When the solution initial pH was increased from 2.4 to 9.0, dye uptake increased from 13.78 to 43.75 mg/g. It was evident that dye uptake was significantly affected by the solution pH. This behavior could be explained with reference to the zero point charge of the material. Zero point charge of a material is the solution pH at which the adsorbent exhibits a net zero surface charge in the absence of any specific adsorption. In the present study, zero point charge was determined by using the powder addition method.[29] pH_{zpc} was found to be 7.5 (Figure 1).

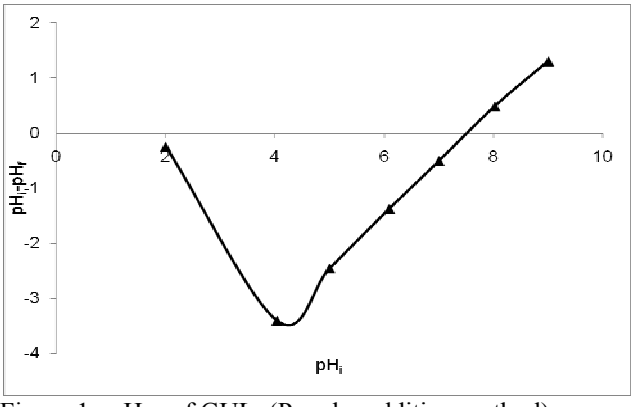

Figure 1. pH_{zpc} of GUL. (Powder addition method)

Thus, at a pH below 7.5 (pH_{zpc}), sorbent surface was likely to have a net positive charge and, therefore, adsorption of cationic dye was low. On the other hand, when solution pH was greater than 7.5, the adsorbent surface was likely to have a net negative charge which favored adsorption of cationic dyes. Similar trends were observed by Kumar and Porkodi (2007),[29] Bulut and Aydin (2006),[30] and Kumar and Kumaran (2005)[31] during adsorption of MB on different adsorbents. Since the optimum pH was close to the natural solution pH, for further studies pH was not adjusted.

The transient behavior of adsorption could be well explained by second order kinetic model ($R^2 > 0.92$). Second order rate constants and maximum specific uptakes predicted by Ho's pseudo second order model at different initial pH values are presented in Table 1.

Table 1. Effect of pH on adsorption of MB onto GUL. (D = 2 mg/L, d_p = 125 μm, C_o = 100 mg g^{-1}, 150 RPM, T = 303 K)

pH	K_2, g mg^{-1} min^{-1}	$q_{m,\,pre}$ mg g^{-1}	$q_{m,\,exp}$ mg g^{-1}	R^2
2.40	0.000700	20.481	13.78	0.9222
4.00	0.001773	39.323	37.98	0.9551
6.00	0.002332	45.130	42.55	0.9957
8.00	0.002150	46.019	42.70	0.9958
9.00	0.003589	45.548	43.75	0.9984

3.2. Effect of initial concentration

The effect of initial dye concentration on adsorption of MB onto GUL is illustrated in Figures 2 to 4.

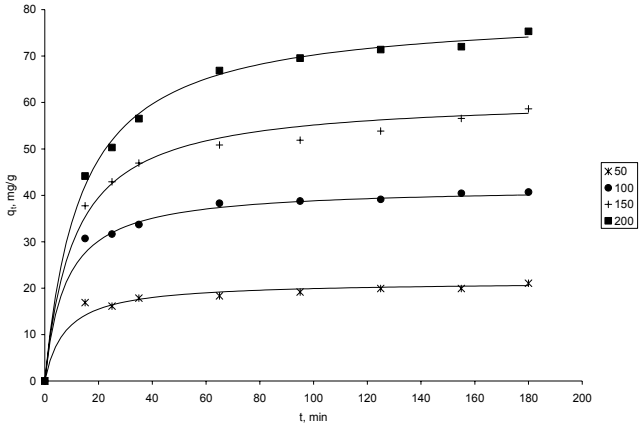

Figure 2. Effect of initial concentration on adsorption of MB onto GUL. (Particle size = 125 μm; RPM = 150; T = 303 K; C_0 = 50 to 200 mg/L; D = 2 g/L)

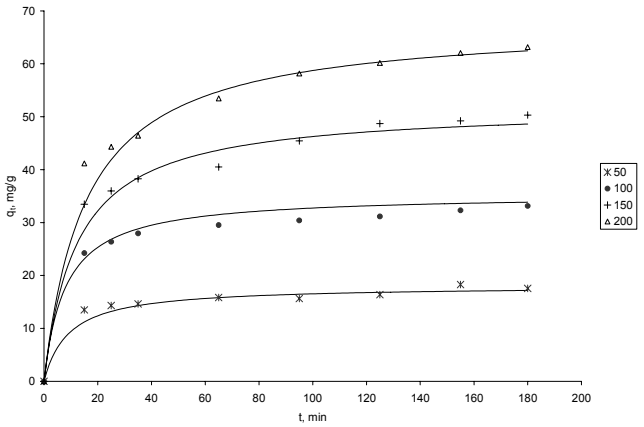

Figure 3. Effect of initial concentration on adsorption of MB onto GUL. (Particle size = 125 μm; RPM = 150; T = 313 K; C_0 = 50 to 200 mg/L; D = 2 g/L)

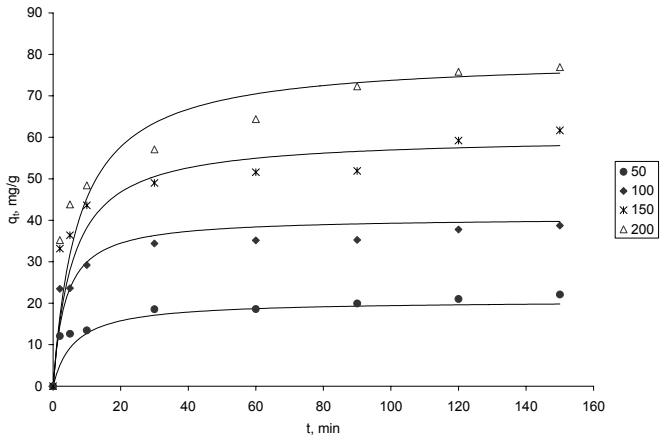

Figure 4. Effect of initial concentration on adsorption of MB onto GUL. (Particle size = 125 μm; RPM = 150; T = 323 K; C_0 = 50 to 200 mg/L; D = 2 g/L)

The pseudo-second order model fits the data well ($R^2 > 0.99$). Values of pseudo-second order kinetic parameters, K_2 & q_e, along with coefficients of determination are given in Table 2. K_2 decreased with increase in initial concentration, while q_e increased with increase in concentration. The dependencies of K_2 and q_e with C_0 can be expressed by the following correlations:

$$K_2 = \frac{C_0}{aC_o^2 + bC_0 + c} \qquad (9)$$

$$q_e = \frac{C_0}{a' + b'C_0} \qquad (10)$$

Table 2. Effect of concentration on adsorption of MB onto GUL.							
	Pseudo-second order model				Intra-particle diffusion model		
T, K	C_o mg/g	K_2, g mg^{-1} min^{-1}	$q_{e,pre}$ mg/g	R^2	K_i mg g^{-1} min$^{-0.5}$	I, mg g^{-1}	R^2
303	50	0.0061	21.33	0.9973	0.45	14.73	0.930
303	100	0.0031	42.21	0.9995	1.87	22.89	0.975
303	150	0.0014	60.70	0.9972	3.06	27.13	0.940
303	200	0.0009	79.77	0.9991	5.45	23.33	0.996
313	50	0.0060	18.37	0.9933	0.38	11.97	0.915
313	100	0.0036	33.97	0.9985	1.23	19.99	0.937
313	150	0.0014	53.49	0.9966	1.66	27.55	0.952
313	200	0.0011	67.26	0.9986	2.93	29.60	0.995
323	50	0.0078	22.15	0.9955	1.19	11.14	0.941
323	100	0.0068	38.77	0.9976	2.89	18.79	0.943
323	150	0.0028	61.23	0.9905	3.93	28.46	0.936
323	200	0.0046	68.05	0.9995	5.04	30.64	0.940

Values of the coefficients in these equations determined by non-linear regression are listed in Table 3. High R^2 (> 0.99) implies that the correlations fit well with the experimental data. By substituting the Eqs. 9 and 10 in Eq. 6, it is possible to predict the kinetics of MB adsorption onto GUL for any unknown initial concentration in the range of 50 to 200 mg/dm^3. Figures 2 to 4 illustrate the comparison of the predicted data with the experimental data. Slopes and intercepts of the intra-particle diffusion plots at various concentrations are given in Table 2. It can be observed that the intercept values increase with increase in initial dye concentration of the solution. The greater the intercept value, the higher is the boundary layer thickness. Similar observations were earlier made by Mane et al. (2007).[6] Thus, it is evident from the observation that the boundary layer effects are predominant at higher initial dye concentration.

Table 3. Coefficients of predictions models (Eqs. 9 & 10) for k_2 and q_e.							
	k_2				q_e		
T, K	A	b	C	R^2	a'	b'	R^2
303	8.851	-849	28545	0.9999	0.0012	2.272	0.9999
313	9.521	-1033	36131	0.9979	0.0012	2.710	0.9983
323	5.808	-705	27135	0.9995	0.0007	2.392	0.9981

3.3. Effect of particle size

Effect of particle size is shown in Figure 5. The effect of particle size on the removal of MB was studied by using four different size particles (40, 125, 230, and 548 μm) keeping all other parameters constant (C_0 = 200 mg/dm^3, T = 303 K, agitation speed = 150 RPM, pH = 7, D = 2 g/L). The specific uptake of dye increased from 33.12 to 63.88 mg/g when particle size decreased from 548 to 40 microns.

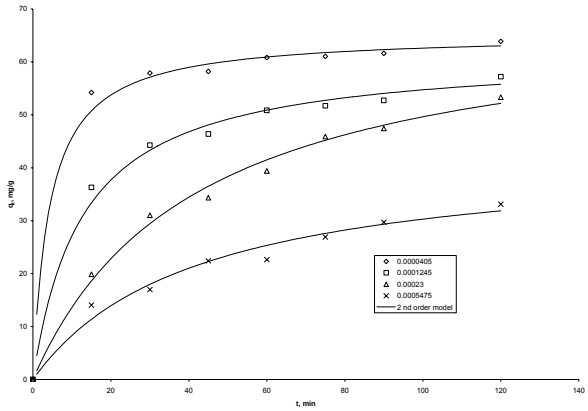

Figure 5. Effect of particle size on adsorption of MB onto GUL. (pH = 7; RPM = 150; T = 303 K; C_0 = 200 mg/L; D = 2 g/L)

An increase in uptake with decreasing particle size can be ascribed to adsorption being limited to the external surface area of the adsorbent, as small particles have a larger external surface area.[32] For smaller particles, equilibrium was achieved much more rapidly, while equilibrium was reached slowly with larger particles. This may be due to the fact that dye molecules may take a longer time to reach the adsorption site. The pseudo-second order model explained the kinetics well (R^2 > 0.96). Second order rate constants and maximum specific uptakes predicted by Ho's pseudo-second order model are presented in Table 4.

Table 4. Effects of particle size on adsorption of MB onto GUL.				
	Pseudo-second order model			
d_p, μm	K_2, g mg^{-1} min^{-1}	$q_{m,\ pre}$ mg g^{-1}	$q_{m,\ exp}$ mg g^{-1}	R^2
40	0.003566	65.301	63.880	0.9990
125	0.001272	61.703	57.220	0.9960
230	0.000342	70.281	53.345	0.9870
548	0.000559	42.921	33.118	0.9599

Second order rate constant decreased with increase in size. These observations are in agreement with those of Qada *et al*. (2006),[32] Ho and McKay (1999),[33] and Poots *et al*. (1976).[34]

The following empirical relationships fit the experimental data.

$$q_e = 65.92 - 59535\ d_p,\ R^2 = 99.4 \quad (11)$$

$$\log K_2 = -5.954 - 0.7792 \log d_p,\ R^2 = 87.7 \quad (12)$$

3.4. Effect of adsorbent dosage

The effect of dosage of GUL on the removal of MB is shown in Figure 6.

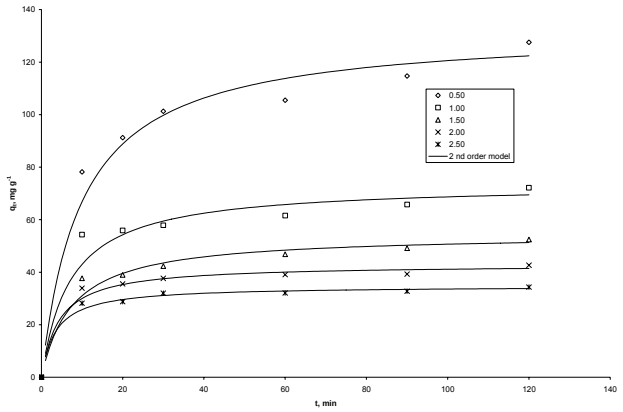

Figure 6. Effect of adsorbent dosage on adsorption of MB onto GUL. (pH = 7; RPM = 150; T = 303 K; C_0 = 100 mg/L; Particle size = BSS# -100+150)

At higher adsorbent dosage, uptakes were essentially the same. An increase in adsorbent dosage increases the surface area available for adsorption; therefore, percentage dye removal increases with increase in adsorbent dosage. The results are given in Table 5.

Table 5. Effects of particle dosage on adsorption of MB onto GUL.

	Pseudo-second order model			
D mg L^{-1}	K_2, g mg^{-1} min^{-1}	$q_{m,\,pre}$ mg g^{-1}	$q_{m,\,exp}$ mg g^{-1}	R^2
0.5	0.000769	132.403	127.550	0.9912
1	0.001909	73.577	72.175	0.9925
1.5	0.002424	54.512	52.457	0.9969
2	0.005399	42.914	42.650	0.9964
2.5	0.008220	34.764	34.330	0.9987

Dye uptake was significantly higher when the dosage was 0.5 g/L, and nearly constant at higher dosages. When excess adsorbent dosage is used, a significant portion of the adsorption sites remain unsaturated. This obviously leads to low specific adsorption capacity. When the adsorbent dosage was lowered, the number of active sites saturated with dye increased; therefore, specific uptake also increased. Meanwhile, with increase in adsorbent dosage, K_2 increased. Second order rate constants and maximum specific uptakes predicted by Ho's pseudo second order model are presented in Table 5. It was observed that q_m and K_2 have a logarithmic relationship with adsorbent dosage. Similar trends have been reported by Ho and Ofomaja (2006),[35] Ho *et al.* (1995),[36] and Ponnusami *et al.* (2007; 2008a; 2008b).[37, 38, 39] The mathematical relationship between K_2, q_e, and adsorbent dosage can be expressed as follows:

$$\log K_2 = -2.724 + 1.424 \log D \quad R^2 = 95.7\% \qquad (13)$$

$$\log q_e = 1.874 - 0.8201 \log D \quad R^2 = 99.9\% \qquad (14)$$

High correlation coefficients indicate the validity of the empirical expressions.

3.5. Effect of agitation

The effect of agitation was studied by varying RPM from 50 to 200. The initial concentration was 200 mg/L. As expected, equilibrium dye concentration in the solid phase was not affected by agitation speed. However, at higher agitation speed equilibrium was reached more rapidly as compared to low speed agitation. The effect of agitation on adsorption of MB on GUL is illustrated in Figure 7.

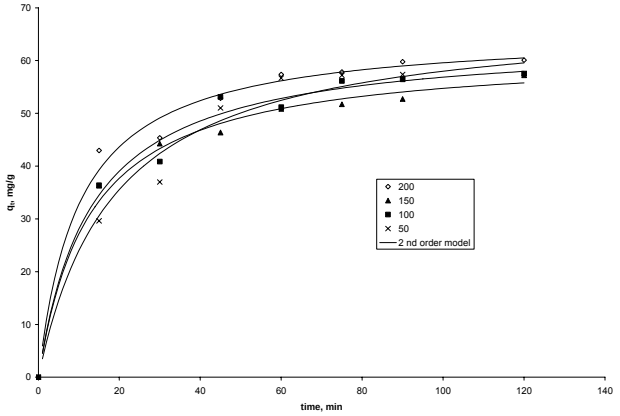

Figure 7. Effect of agitation speed on adsorption of MB onto GUL. (pH = 7; T = 303 K; C_0 = 200 mg/L; D = 2 g/L; Particle size = BSS# -100+150)

Second order rate constant increased from 7.75E-4 to 15.18E-4 when RPM was increased from 50 to 200. Determined pseudo-second order kinetic model parameters and intra-particle model parameters are presented in Table 6 along with regression coefficients.

Table 6. Effect of agitation speed on adsorption of MB onto GUL.

	Pseudo-second order model				Intra-particle diffusion model		
RPM min^{-1}	K_2, g mg^{-1} min^{-1}	$q_{m,\,pre}$ mg g^{-1}	$q_{m,\,exp}$ mg g^{-1}	R^2	K_i	I	R^2
50	0.000775	68.851	57.530	0.9835	0.011	57.300	0.975
100	0.001210	64.178	57.530	0.9945	0.054	56.348	0.978
150	0.001272	61.703	57.220	0.9960	1.325	41.769	0.971
200	0.001518	65.569	60.088	0.9973	5.645	5.406	0.914

It can be seen that with increase in agitation speed, external film thickness decreased. This confirmed that increase in agitation speed helped to overcome the external film transfer resistances.

3.6. Equilibrium study

Figures 8, 9, and 10 present the isotherms at 293, 303, and 313 K, respectively, for the adsorption of MB onto GUL. The Langmuir model best fits the experimental data within this temperature range.

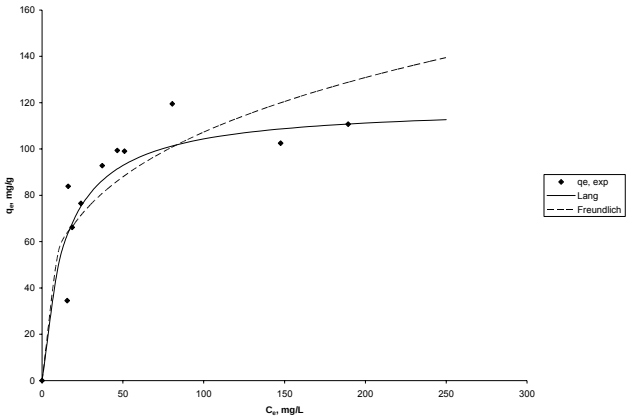

Figure 8. Equilibrium plot of MB adsorption onto GUL. (pH = 7; T = 293 K; D = 1 g/L; RPM = 150; Particle size = BSS# -100+150)

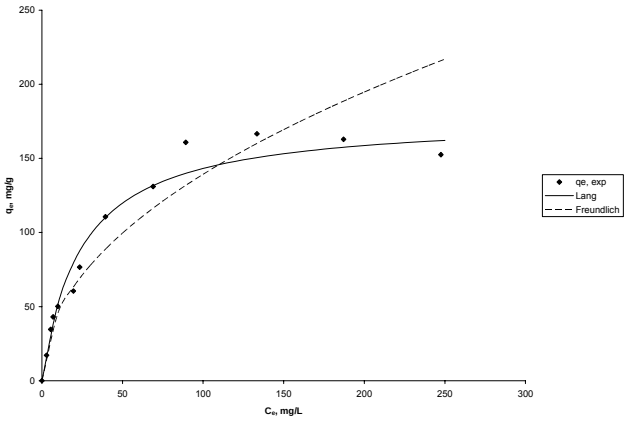

Figure 9. Equilibrium plot of MB adsorption onto GUL. (pH = 7; T = 303 K; D = 1 g/L; RPM = 150; Particle size = BSS# -100+150)

The isotherm parameters along with the regression coefficients are given in Table 7. The monolayer adsorption capacity of GUL was found to be 120, 178, and 253 mg/g at temperatures of 293, 303, and 313 K, respectively. These values are much higher than that of many other low cost adsorbents found in the literature (Table 8). The fact that Langmuir adsorption fits the data well may be due to the homogenous distribution of active sites on the adsorbent surface.[30] Dimensionless constant separation factor, $R_{L,}$ was determined using the Langmuir isotherm constant. Values of R_L were found to be in the range of 0.053 to 0.584, 0.088 to 0.708, and 0.169 to 0.836 at temperatures of 293, 303, and 313 K, respectively. This indicated that the adsorption of MB onto GUL was favorable. The value of n, the Freundlich parameter, which was between 1 and 10 (1.727, 2.067, 2.809) also confirmed that the adsorption was favorable.

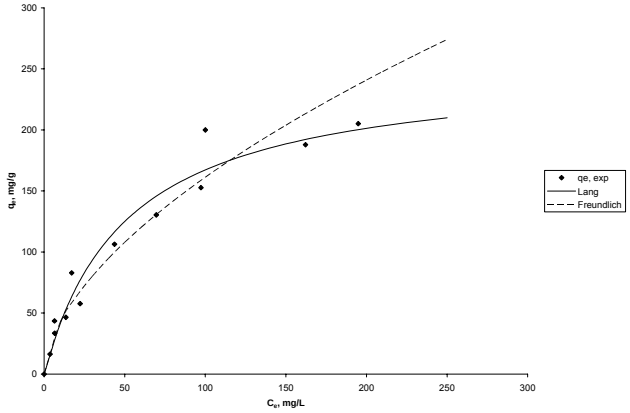

Figure 10. Equilibrium plot of MB adsorption onto GUL. (pH = 7; T = 313 K; D = 1 g/L; RPM = 150; Particle size = BSS# -100+150)

Table 7. Isotherm parameters for adsorption of MB onto GUL.

	Langmuir		Freundlich	
293 K	$K_{L,}$ dm^3 mg^{-1}	0.0712	$K_{F,}$ $(mg\ g^{-1})*$ $(dm^3/\ mg)^{1/n}$	21.22
	$q_{m,}$ mg/g	120.0	n	2.809
	R^2	0.9707	R^2	0.5116
	χ^2	24.20	χ^2	30.57
303 K	$K_{L,}$ dm^3 mg^{-1}	0.0413	$K_{F,}$ $(mg\ g^{-1})*$ $(dm^3/\ mg)^{1/n}$	15.00
	$q_{m,}$ mg/g	177.9	n	2.067
	R^2	0.9857	R^2	0.9300
	χ^2	12.00	χ^2	40.52
313 K	$K_{L,}$ dm^3 mg^{-1}	0.0196	$K_{F,}$ $(mg\ g^{-1})*$ $(dm^3/\ mg)^{1/n}$	11.21
	$q_{m,}$ mg/g	252.7	n	1.727
	R^2	0.9485	R^2	0.9358
	χ^2	30.69	χ^2	35.53

Table 8. Comparison of reported adsorption capacities of various adsorbents for methylene blue.	
Adsorbent	q_{max}, mg/g
Fly ash	13.42[40]
Rice husk	40.58[41]
Cotton waste	278[42]
Untreated guava leaves	295[39]
Neem leaf	8.76 – 19.61[5]
Banana peel	20.8[43]
Orange peel	18.6 [43]
Wheat shells	16.56-21.50[29]
GUL	120 - 253, present study

3.7. Thermodynamic study

The values of ΔG were calculated using Eq. 7. A plot of ln K_L vs. 1/T was a straight line (Figure 11).

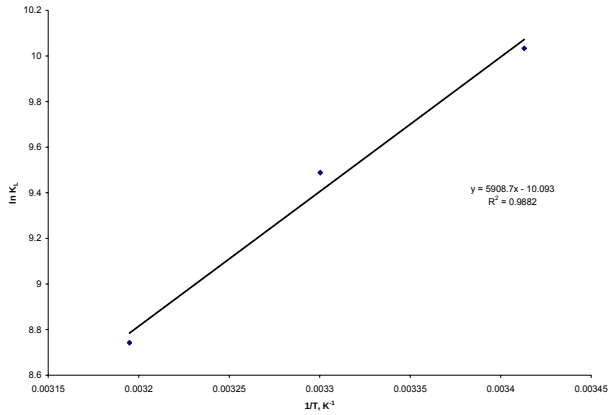

Figure 11. Van't Hoff plot for MB adsorption onto GUL.

From the slope and intercept, ΔH and ΔS were calculated. Results are shown in Table 9.

Table 9. Thermodynamic parameters.				
T, K	Δ G, kJ/mol	Δ H, kJ/mol	Δ S, kJ/mol	R^2
293	-24.44	-49.12	-0.084	98.82%
303	-23.90			
313	-22.75			

Gibbs free energy values were found to be -24.44, -23.90, and -22.75 kJ/mol, respectively, at 293, 303, and 313 K. Negative values of ΔG indicated that the adsorption process is spontaneous. The value of ΔH was -49.12 kJ/mol, which was in the range of chemisorption. The negative value of ΔH also indicated that the adsorption process is exothermic. Values of q_m were predicted to be 120, 178, and 253 at 293, 303, and 313 K, respectively. The increase in q_m with increase in temperature also confirms that MB adsorption on GUL is an exothermic process. Meanwhile, the ΔS value was found to be negative (-0.084 kJ/mol). The negative value of ΔS indicated that the MB molecules are more regularly arranged (decrease in randomness) on the adsorbent surface.[44-46]

4. Conclusions

Based on the experimental results, the following conclusions can be made:

1. GUL has shown excellent adsorption potential compared to many other non-conventional adsorbents. Therefore, it can serve as an attractive low-cost alternate for costly activated carbon.
2. The Langmuir and Freundlich isotherm parameters confirmed that the adsorption of MB on GUL was favorable.
3. Adsorption of MB on GUL was favored by increase in pH, concentration, temperature, speed of agitation, decrease in adsorbent dosage, and particle size.
4. The Langmuir isotherm model and Ho's pseudo-second order model were found to be the best fitting isotherm and kinetic models.
5. Thermodynamic analysis indicated that the adsorption of MB onto GUL was:
   i. Exothermic (ΔH was negative, -49.12 kJ/mol);
   ii. Chemisorption (ΔH > 30 kJ/mol, -49.12 kJ/mol);
   iii. Feasible and Spontaneous (ΔG = -24.44, -23.90, -22.75 kJ/mol); and
   iv. Decreased randomness on the solid surface (Δ S = - 0.084 kJ/mol).

5. Nomenclature

C_0 initial dye concentration in aqueous solution (mg/dm^3)

C_e equilibrium dye concentration in liquid phase (mg/dm^3)

D adsorbent dosage (g/dm^3)

d_p particle size (μm)

K_2 pseudo-second order rate constant ($g\ mg^{-1}\ min^{-1}$)

K_F Freundlich constant ($mg\ g^{-1}$)($dm^3/\ mg$)$^{1/n}$

K_L Langmuir adsorption constant ($dm^3\ mg^{-1}$)

1/n Freundlich parameter

q_e equilibrium dye concentration in solid phase ($mg\ g^{-1}$)

q_m maximum dye adsorbed per unit mass of adsorbent ($mg\ g^{-1}$)

R the gas universal constant (8.314 J/mol K)

R_L Langmuir separation or equilibrium parameter (dimensionless)

RPM speed of agitation, min^{-1}

T absolute temperature (K)

t time (min)

ΔG free energy of adsorption (kJ mol^{-1})

ΔH change in enthalpy (kJ mol^{-1})

ΔS change in entropy (kJ mol^{-1} K^{-1})

Greek symbol

χ^2 chi square

6. References

1. Nacera Yeddou and Aicha Bensmalli, (2005) Kinetic models for the sorption of dye from aqueous solution by claywood sawdust mixture. Desalination;185:499-508.
2. Renmin Gong, Youbin Jin, Jian Chen, Yun Hu and Jin Sun, (2007) Removal of basic dyes from aqueous solution by sorption on phosphoric acid modified rice straw, Dyes Pigments;73:332-337.
3. J.M., Chern., S.N., Huang. (1998) Study of nonlinear wave propagation theory: 1. Dye adsorption by activated carbon. Ind Eng Chem Res;37:253-257.
4. M. Ozacar, and IA. Sengil. (2003) Adsorption of reactive dyes on calcined alunite from aqueous solutions. J Hazard Mater B;98:211-224.
5. K.G. Bhattacharyya, A. Sharma, (2005) Kinetics and thermodynamics of methylene blue adsorption on Neem (*Azadirachta Indica).* Dyes Pigments;65:51–59.
6. V.S. Mane, I.D. Mall, V.C. Srivastava, (2007) Use of bagasse fly ash as an adsorbent for the removal of brilliant green dye from aqueous solution. Dyes Pigments;73:269-278.
7. Y. S. Ho, Wen-Ta Chiu, Chung-Chi Wang, (2005) Regression analysis for the sorption isotherms of basic dyes on sugarcane dust. Biores Technol;96:1285-1291.
8. T. G. Chuah, A. Jumasiah, I. Azni, S. Katayon, S.Y. Thomas Choong, (2005) Rice husk as a potentially low-cost biosorbent for heavy metal and dye removal: an overview. Desalination;175:305-316.
9. C. Namasivayam, D. Prabha, M. Kumutha, (1998) Removal of direct red and acid brilliant blue by adsorption on to banana pith. Biores Tech;64:77-79.
10. C. Namasivayam, M. Dinesh Kumar, K. Selvi, R. Ashruffunissa Begum, T. Vanathi, R. T. Yamuna, (2001) 'Waste' coir pith—a potential biomass for the treatment of dyeing wastewaters. Biomass Bioenergy;21:477-483.
11. F. Doulati Ardejani, Kh. Badii, N. Yousefi Limaee, N.M. Mahmoodi, M. Arami, S.Z. Shafaei, A.R. Mirhabibi, (2007) Numerical modelling and laboratory studies on the removal of Direct Red 23 and Direct Red 80 dyes from textile effluents using orange peel, a low-cost adsorbent. Dyes Pigments; 73: 178-185.
12. Haluk Aydin, Gulay Baysal, (2006) Adsorption of acid dyes in aqueous solutions by shells of bittim (Pistacia khinjuk Stocks). Desalination;196:(1-3), 248-259.
13. D. K. Singh, B. Srivastava, (1999) Removal of basic dyes from aqueous solutions by chemically treated Psidium gujava leaves. Indian J Environ Hlth;41: 333-45.
14. Runping Han, Weihua Zou, Weihong Yu, Shujian Cheng, Yuanfeng Wang and Jie Shi, (2007) Biosorption of methylene blue from aqueous solution by fallen phoenix tree's leaves. J Hazard Mater;141:156-162
15. Hameed, B.H., Mahmoud, D.K., Ahmad, A.L. (2008) Sorption of basic dye from aqueous solution by pomelo (Citrus grandis) peel in a batch system. Colloids Surf A: Physicochemical Engineering Aspects; 316 (1-3): 78-84
16. Shaobin Wang, Huiting Li, (2007) Kinetic modeling and mechanism of dye adsorption on unburned carbon. Dyes Pigments;72 (3):308-314.
17. I., Langmuir, (1916) The constitution and fundamental properties of solids and liquids. J Am Chem Soc;38(11): 2221-2295.
18. Z. Eren, and F. Nuran Acar, (2006) Adsorption of Reactive Black 5 from an aqueous solution: equilibrium and kinetic studies. Desalination; 194: 1-10.
19. H.M.F., Freundlich, (1906) Űber die adsorption in lősungen. Zeitschrift fűr Physikalische Chemie; 57: 385-470.
20. P. K. Malik, (2004) Dye removal from wastewater using activated carbon developed from sawdust: adsorption equilibrium and kinetics. J Hazard Mater;113:81-88.
21. Ho, Y. S., Wang, C. C., (2004) Pseudo-isotherms for the sorption of cadmium ion onto tree fern. Proc Biochem; 39 (6): 761-765.
22. Ho, Y. S., (2004) Selection of optimum sorption isotherm. Carbon; 42(10): 2115-2116.

23. Lagergren, S., (1898) Zur theorie der sogenannten adsorption gelöster stoffe, Kungliga Svenska Vetenskapsakademiens. Handlingar; 24 (4): 1-39.
24. Ho, Y.S. and McKay, G., (2000) The kinetics of sorption of divalent metal ions onto sphagnum moss peat. Water Research; 34 (3): 735-742.
25. Ho, Y.S. and McKay, G., (1999) Pseudo-second order model for sorption processes. Proc Biochem; 34 (5): 451-465.
26. Ho, Y.S. and McKay, G., (1998) Sorption of dye from aqueous solution by peat. Chem Eng J; 70 (2): 115-124.
27. Ho Y.S., Wase D. A. J., Forster C. F. (1996) Kinetic studies of competitive heavy metal adsorption by sphagnum moss peat. Environ Tech; 17 (1): 71-77.
28. Weber, W. J., & Morris, J. C., (1963) Kinetics of adsorption on carbon from solution. J Sanit Eng Div ASCE; 89: 31-35.
29. K. Vasanth Kumar, K. Porkodi, (2007) Mass transfer, kinetics and equilibrium studies for the biosorption of methylene blue using *Paspalum notatum.* J Hazard Mater; 146 (1-2): 214-226.
30. Y. Bulut and H. Aydin, (2006) A kinetic and thermodynamic study of MB on wheat shell. Desalination; 194: 259-267.
31. K. Vasanth Kumar & A. Kumaran (2005) Removal of methylene blue by mango seed kernel powder. Biochem Eng; J 27: 83-93.
32. N. Emad, El Qada, Stephan J. Allen, Gavin M. Walker, (2006) Adsorption of Methylene Blue onto activated carbon produced from steam activated bituminous coal: study of equilibrium adsorption isotherm. Chem Eng J; 124: 103-110.
33. Y. S., Ho, and G., McKay, (1999) A kinetic study of dye adsorption by biosorbent waste product pith. Resour Conserv Recycling; 25: 171-193.
34. V. J. Poots, G. McKay, J. J. Healy, (1976) The removal of acid dye from effluent using natural adsorbent – I peat. Wat res; 10: 1061-1066.
35. Y.S. Ho, A.E. Ofomaja, (2006) Pseudo-second-order model for lead ion sorption from aqueous solutions onto palm kernel fiber. J Hazard Mater; 129 (1-3): 137-142.
36. Y. S. Ho, D. A. J. Wase, C. F. Forster, (1995) Batch nickel removal from aqueous solution by sphagnum moss peat. Wat Res; 29 (5): 1327-1332.
37. V. Ponnusami, V. Krithika, R. Madhuram, S.N. Srivastava, (2007) Biosorption of reactive dye using acid-treated rice husk: Factorial design analysis. J Hazard Mater; 142 (1-2): 397-403.
38. V. Ponnusami, R. Madhuram, V. Krithika, S.N. Srivastava, Effects of process variables on kinetics of methylene blue sorption onto untreated guava (*Psidium guajava*) leaf powder: Statistical analysis. Chem Eng J; 140(1-3): 609-613.
39. V. Ponnusami, S. Vikram, S.N. Srivastava, (2008) Guava (Psidium guajava) leaf powder: Novel adsorbent for removal of methylene blue from aqueous solutions. J Hazard Mater; 152 (1): 276-286.
40. S. Wang, Y. Boyjoo and A. Choueib, (2005) A comparative study of dye removal using fly ash treated by different methods. Chemosphere;60:1401-1407.
41. V. Vadivelan, K.V. Kumar, (2005) Equilibrium, kinetics, mechanism, and process design for the sorption of methylene blue onto rice husk. J Coll Interface Sci; 286: 90-100.
42. McKay, G., Porter, J.F., Prasad, G.R., (1999) The removal of dye colours from aqueous solutions by adsorption on low-cost materials. Water Air Soil Pollut; 114: 423-438.
43. G. Annadurai, J. Ruey-shin, L. Duu-Jong (2002) Use of cellulose-based waste for adsorption of dyes from aqueous solutions. J Hazard Mater; B92:263-274.
44. Augustine E. Ofomaja, Yuh-Shan Ho, (2007) Equilibrium sorption of anionic dye from aqueous solution by palm kernel fibre as sorbent. Dyes Pigments;74 (1): 60-66.
45. E. Eren, B. Afsin, (2008) Investigation of a basic dye adsorption from aqueous solution onto raw and pre-treated bentonite surfaces. Dyes Pigments;76(1): 220-225.
46. E. Eren, B. Afsin, (2007) Investigation of a basic dye adsorption from aqueous solution onto raw and pre-treated sepiolite surfaces. Dyes Pigments;73(2): 162-167.